INSTITUTE OF PHYSICS PUBLISHING JOURNAL OF PHYSICS B: ATOMIC, MOLECULAR AND OPTICAL PHYSICS

J. Phys. B: At. Mol. Opt. Phys. **38** (2005) S333–S342 doi:10.1088/0953-4075/38/2/024

Ionization due to the interaction between two Rydberg atoms

F Robicheaux

Department of Physics, Auburn University, Auburn, AL 36849-5311, USA

E-mail: robicfj@auburn.edu

Received 30 June 2004
Published 5 January 2005
Online at stacks.iop.org/JPhysB/38/S333

Abstract

Using a classical trajectory Monte Carlo method, we have computed the ionization resulting from the interaction between two cold Rydberg atoms. We focus on the products resulting from close interaction between two highly excited atoms. We give information on the distribution of ejected electron energies, the distribution of internal atom energies and the velocity distribution of the atoms and ions after the ionization. If the potential for the atom is not purely Coulombic, the average interaction between two atoms can change from attractive to repulsive giving a Van de Graaff-like mechanism for accelerating atoms. In a small fraction of ionization cases, we find that the ionization leads to a positive molecular ion where all of the distances are larger than 1000 Bohr radii.

1. Introduction

Two Rydberg atoms can strongly interact at large distances due to the size and easily perturbed nature of highly excited states. A gas of cold Rydberg atoms can exhibit interesting many-body effects originating from dipole–dipole or van der Waals interactions between the atoms. For heavy atoms, e.g. Rb or Cs, at low temperatures, the velocities and accelerations are low enough that the atoms can be treated as fixed in space over a time of approximately 1 μs. For principle quantum number, n, less than $\sim$100, the internal quantum states of the atoms can be described within an essential states model if the atoms are separated by more than $10n^2\,a_0$, approximately three atomic diameters. In an essential states model, only states within an n-manifold or only states with near resonance transitions strongly interact.

At longer times, the atoms can be attracted to each other through long-range forces. There is nothing to prevent the atoms from coming together. When the atoms are close enough, one electron can drop to more deeply bound levels while the other electron is ionized. This process can be symbolically written as

$$\mathrm{Ryd}(n) + \mathrm{Ryd}(n) \rightarrow \mathrm{Ryd}(n') + \mathrm{ion} + \mathrm{electron}. \quad (1)$$

0953-4075/05/020333+10$30.00

This effect was observed in cold Rydberg collisions [1–4]. The cross section for ionization at somewhat higher energy was investigated in [5]. Reference [6] noted that polarization affected the cross section even in collisions between a Rydberg atom and an atom in a low excited state. Reference [7] performed approximate quantum calculations of the ionization from the interaction between several Rydberg atoms.

In the present paper, we extend the investigation of [5] to treat much lower translational energies and provide information on the products that result from close Rydberg–Rydberg interaction. This information may be useful for understanding the limitations of cold Rydberg gases as coherent quantum systems since the presence of relatively fast positive ions and slow electrons will cause a rapid decoherence of the gas.

A quantum-mechanical investigation of the strong interaction between two Rydberg atoms is beyond current capabilities. The treatment of [7] provides a qualitative estimate of rates when the atoms are sufficiently far apart that perturbative quantum decay is the most important mechanism. However, a classical treatment of this system should be accurate when the atoms are in highly excited states. Therefore, we have utilized a classical trajectory Monte Carlo method (CTMC) in this investigation. The CTMC method solves Hamilton's equations for the system starting from a distribution of trajectories whose starting conditions mimic a quantum system. The CTMC method should be accurate so long as quantum interference effects are unimportant and the processes are not classically forbidden; both of these conditions are probably satisfied for strongly interacting Rydberg atoms.

The main limitation of the current treatment is in the choice of initial conditions for the atoms. I have chosen to investigate atoms that have a random distribution of ℓ, m. This situation will occur in ultracold plasmas and in Rydberg gases that have been disturbed by blackbody radiation or charged particles. Unfortunately, this choice of initial conditions does not apply to a wide variety of interesting situations. In many experiments, the atoms will all be in low angular momentum states. Low angular momentum states overlap the core electrons and have energies that can be substantially shifted from the degenerate n-manifold. The classical analogue of this is the precession of the Runge–Lenz vector due to a short-range non-Coulomb potential. The long-range interaction between two atoms in low angular momentum states will depend strongly on the type of states and the type of atoms. However, the Rydberg–Rydberg interaction will cause an ℓ, m mixing when the atoms are close enough. Thus, it seems likely that the choice of initial conditions will not qualitatively affect the results of this investigation.

In all of the calculations, the two Rydberg atoms are initially at an energy equivalent to an $n = 60$ state of hydrogen. The atoms have an initial thermal energy of approximately 500 μK. This n-manifold and thermal temperature were chosen to be near what could be obtained experimentally without recourse to extraordinary measures (temperatures of a few hundred μK are routinely obtained in magneto optic traps and the excitation of specific n-states near $n = 60$ requires laser resolution better than $\sim 1/3$ cm^{-1}). Since the binding energy is much larger than the thermal energy, the results of the present calculations should be applicable to other n-manifolds and temperatures by simple scaling arguments. The main restriction will be that the density of final electronic states of the atom is high enough that it can be approximated as a continuum.

Atomic units are used unless explicitly specified otherwise.

2. Time scales

In the simulation, the atoms start in a statistically random ℓ, m state in the $n = 60$ manifold. The Rydberg period for a trajectory is $\sim$33 ps. Thus, approximately 30 000 radial oscillations

occur if atoms require 1 μs to reach the strong interaction region. In the numerical simulation we describe below, we solve Hamilton's equations using the full electrostatic interaction forces, but we use the asymptotic form of the interaction for the estimates of this section.

An estimate of the time for the atoms to reach the strong interaction region can be obtained from the asymptotic form of the potential which arises from the dipole–dipole interaction: $V_{\rm asym} = -d^2/R^3$ where $d \sim n^2$ is roughly the dipole moment of the atom. The initial atom velocity is approximately 0, so the radial inter-atom velocity at a separation R is approximately equal to

$$v = \sqrt{2d^2(2/M)\left(\frac{1}{R^3} - \frac{1}{R_0^3}\right)} \tag{2}$$

where M is the mass of an atom and R_0 is the starting separation of the atoms. The time for the strong interaction to commence is approximately

$$T = \int_0^{R_0} \frac{1}{v(R)}\,{\rm d}R = \sqrt{\frac{MR_0^5}{4d^2}}\int_0^1 \sqrt{\frac{x^3}{1-x^3}}\,{\rm d}x \tag{3}$$

where the integral equals $\sqrt{\pi}\,\Gamma(5/6)/\,\Gamma(1/3) \simeq 0.75$. The time to come together can be simplified to

$$T \sim 20\ \mu{\rm s} \times \sqrt{M({\rm amu})R_0^5(\mu{\rm m})/n^2}. \tag{4}$$

For Rb in $n = 60$ the time is approximately 1 μs for a separation of 3 μm. For H in $n = 60$, the time is approximately 0.1 μs for a separation of 3 μm. Atoms with a separation of 3 μm have a density of approximately 4×10^{10} cm^{-3}. For these parameters, $k_BT/(d^2/R^3) \sim 1/50$ which agrees with our assumption that the inter-atom potential energy is much greater than the kinetic energy.

3. Numerical method

The simulations treat the four charged particles interacting through Coulomb forces. In the numerical simulation, we use the full electrostatic force between the four charged particles. Since there are only four particles, we do not need to use an asymptotic or multipole expansion to compute the forces between the particles.

Only the hydrogen atom has a pure Coulomb interaction. For quantum calculations, there is a well-defined prescription for including the core electrons in the calculation, but a treatment of non-Coulombic interactions is not well defined for classical calculations. In the present calculations, the interaction between the electrons and nuclei is given by a soft core potential $V(r) = -1/\sqrt{r^2+1}$. Because the atoms are in high-n states, the size of the atom compared to the size of the non-Coulombic region is very small. We found that the results did not noticeably depend on the range of the soft core. The soft core has the added advantage that the acceleration does not diverge which helps in the solution of Hamilton's equations.

Hamilton's equations are solved using a fourth-order Runge–Kutta method with an adaptive step size algorithm. The accuracy condition for the adaptive step size algorithm varies with time. When both atoms are in high angular momentum states, the time step can be relatively large, but the step size must be much smaller when the internal angular momentum of one of the atoms is small because an electron can closely approach a nucleus. The interaction between atoms causes the angular momentum of each atom to precess so a typical trajectory has each atom cycling between high and low angular momentum during each collision. The precession time of the angular momenta is much longer than the Rydberg period.

Since the atoms spend a long time travelling from their initial separation to the point where they strongly interact, we need to preserve the accuracy for both high and low angular momentum trajectories. Unfortunately, the accuracy parameter in the adaptive step size algorithm needs to be much smaller for low angular momentum trajectories to conserve energy. Running every trajectory with the accuracy parameter set for low angular momentum would be prohibitively slow. We implemented a method that adjusted the accuracy parameter with time so that larger step sizes were allowed when both atoms were in high angular momentum states but small step sizes resulted for low angular momentum.

The method for adjusting the energy parameter takes advantage of the fact that the Runge–Kutta propagation scheme does not exactly conserve energy. The accuracy parameter was adjusted in time increments of the Rydberg period, $\tau_{\rm Ryd}$. The accuracy parameter, ε_N, between $N\tau_{\rm Ryd} < t < (N+1)\tau_{\rm Ryd}$ was determined by

$$\varepsilon_N = \varepsilon_{N-1} \times \Delta E/|E_N - E_{N-1}| \tag{5}$$

where E_N is the calculated energy at time $N\tau_{\rm Ryd}$ and ΔE is the maximum estimated energy error during one Rydberg period. For the simulations reported below, we chose $\Delta E = 5 \times 10^{-14}|E_0|$ with E_0 the initial internal energy of one atom. Because the change in energy during one period can sometimes be accidentally small a maximum value for ε_N was set. Typical trajectories resulted in energy errors less than a part in 10^6–10^8 at the end of the trajectory.

It is known that Runge–Kutta algorithms do not conserve the phase space volume during propagation which could bias our calculated final state distributions. To protect against this bias, we ran a distribution with the accuracy parameter set to be uniformly a factor of 10 smaller than for what we believed to be a converged calculation and found our final state distribution to be unchanged. To check for bias due to numerical round off errors, we computed the final state distribution using two times double precision accuracy and found our final state distribution to be unchanged. As a final and very stringent check, we used a symplectic propagator to solve Hamilton's equations. The symplectic propagator is exactly time reversible, conserves the phase-space volume and should protect against bias of the final state distributions. Again we found the final state distribution to be unchanged within the statistical errors of the Monte Carlo distribution.

4. Fixed nuclei

In a recent paper [8], we performed model quantum calculations of the interaction between two Rydberg atoms. We found that the atoms were remarkably stable. To illustrate this effect in the present calculations, we simulated the interaction between two fixed atoms by freezing the position of the two nuclei. The initial positions and velocities of the electrons were consistent with a random ℓ, m distribution for two separated atoms. For a fixed separation of the nuclei, we then solved Hamilton's equations with the method described above. We stopped the propagation after a fixed time or when one electron moved to distances larger than 15 times the separation between the atoms. If one electron was at a distance larger than 15 times the separation, then that run was counted as ending in ionization. We varied the final time in the simulation from 100 to 2000 times the Rydberg period for one atom.

For a fixed duration, the fraction of trajectories ending in ionization decreased with increasing separation. The range of separations where the fraction of ionization decreased from 90% to 10% was less than $0.5 \times 2n^2\, a_0$ for durations longer than 1000 times the Rydberg period. Thus there is a fairly small range of separations for which the two atoms transition from almost never ionizing to almost always ionizing. As the duration of the simulation

increased, the maximum separation where more than 90% of the trajectories led to ionization increased. The maximum separation distance for 90% ionization was $\sim 1.6 \times 2n^2 a_0$ for 400 Rydberg periods, $\sim 1.8 \times 2n^2 a_0$ for 800 Rydberg periods, $\sim 2.1 \times 2n^2 a_0$ for 1200 Rydberg periods. The probability for ionization did not change greatly when increasing the run time from 1200 to 2000 Rydberg periods.

It may be surprising that the atoms can be quite close together and not ionize: the outer turning point for a low angular momentum electron is approximately at $2n^2 a_0$. This may be attributed to the fact that the two electrons repel each other and the classical trajectories would tend to keep them separated. Of course, as the separation between the electrons increases, the effectiveness with which energy can be exchanged between them decreases. The simulations suggest that the ionization is classically forbidden (although it is energetically allowed) when the separation between the atoms is larger than $\sim 3 \times 2n^2 a_0$! Quantum mechanically the process is not forbidden although it will be small; an estimate could be made using Fermi's golden rule [7] with the initial state being two Rydberg states, n, and the final state is one Rydberg atom in state n_f and the other atom in the continuum (positive energy).

This simulation agrees with quantum calculations we performed for a model problem [8]. In this model, the two electrons were restricted to move radially and the potential was given by $-1/r_1 - 1/r_2 + r_1 r_2/R^3$. In the quantum calculations, even transitions to adjacent n-manifolds were suppressed for R greater than $\sim 5 \times 2n^2 a_0$.

5. Free nuclei

We performed a series of simulations where we allowed the nuclei to move freely. In each simulation, the two atoms are initialized separately using a Monte Carlo distribution with the following properties. The relative position and velocity vectors, $\vec{r}_e - \vec{r}_i$ and $\vec{v}_e - \vec{v}_i$ with the subscript e denoting electron and i denoting ion, are chosen to give a microcanonical ensemble with energy $-1/2n^2$. The initial centre of mass velocity of the atoms, $\vec{V} = (m_e\vec{v}_e + m_i\vec{v}_i)/(m_e + m_i)$, was chosen to give a thermal distribution, proportional to $\exp(-[m_e + m_i]V^2/2k_bT)$, at a temperature of 500 μK. The initial separation of the atoms is set to 3 μm which corresponds to a density of $\sim 10^{10-11}$ cm^{-3}.

The microcanonical distribution for a state of energy $-1/2n^2$ can be obtained from five random numbers. The angular momentum is given by $L = \sqrt{x} \cdot n$ where x is chosen from a flat, random distribution $0 \leqslant x \leqslant 1$. The initial radius is chosen to be the outer turning point for the given L; the random distribution in r is achieved by propagating for a random time, τ_{ran}, where τ_{ran} is chosen from a flat, random distribution between 0 and the Rydberg period. The angular part of the distribution is computed in two steps. In the first step, the initial position is in the xz-plane so that $z = R\cos\theta$ with $\cos\theta$ chosen from a flat random distribution between -1 and 1; the initial velocity is chosen so $v = v_0(\cos\theta\sin\phi, \cos\phi, -\sin\theta\sin\phi)$ where ϕ is chosen from a flat random distribution between 0 and 2π. In the second step, the initial positions and velocities are rotated about the z-axis through a random angle chosen from a flat distribution between 0 and 2π.

The thermal distribution of velocities can be obtained using a standard technique for obtaining a Gaussian distribution. For example, if the distribution of the x-component of the velocity is proportional to $\exp\left(-v_x^2/2\bar{v}^2\right)$, then choosing $v_x = \bar{v}\sqrt{-2\ln x_1}\cos(2\pi x_2)$ where x_1 and x_2 are random numbers with a flat distribution between 0 and 1 will give the appropriate distribution. The initial direction of the relative velocity of the two atoms is completely random.

Four different masses were chosen for the atoms in order to investigate the effect that atomic mass could have on the distributions. In terms of the atomic unit of mass, m_e, the

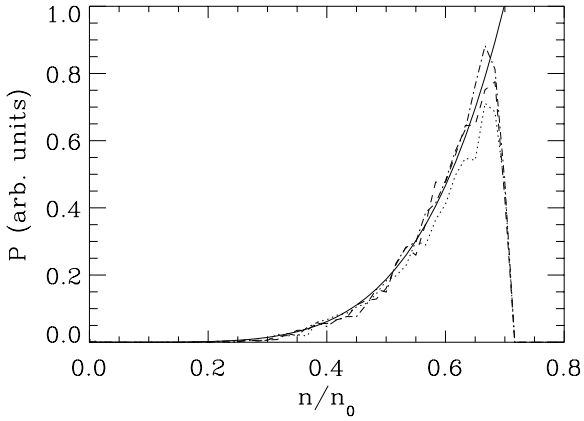

Figure 1. The distribution of n levels of the atom that results after Penning ionization. The distribution is scaled by the initial principal quantum number of the atoms, $n_0 = 60$. The atoms are initially separated by 3 μm and the initial velocity is from a thermal distribution at approximately 500 μK. The dotted line is for two Rb atoms, the dashed line is for two Na atoms and the dash-dot line is for two He atoms. The solid line is proportional to n^5.

masses were $1840 \times m_e$ (H), $4 \times 1840 \times m_e$ (He), $23 \times 1840 \times m_e$ (Na) and $87 \times 1840 \times m_e$ (Rb). The successive masses are roughly separated by a factor of 4 which roughly translates to a factor of 2 in speed. Since the lighter atoms move faster, the duration of the interaction decreases for the lighter atoms. But as will be seen below, the change in mass has relatively little effect on any of the calculated distributions. For clarity, we only plot the results for the three heavier atoms. For each of the atoms, the statistics are based on approximately 20 000 trajectories.

The distributions do not depend strongly on mass because the speed of the atoms is much less than the electron speeds and the duration of the transitions. It might be possible to see larger effects in experiments where the atoms start in low angular momentum states. For low angular momentum, all of the atoms are quite different due to different sets of quantum defects. However, it is unlikely that the difference between the atoms is large.

5.1. Distribution of atomic levels

The conditions for which these calculations will be useful would be when there is a cold gas of Rydberg atoms probably created from a cold gas of atoms excited by a laser pulse. Approximately one-fifth of the trajectories result in ionization for the initial conditions we chose. This shows that a large fraction of the atoms will be ionized on the time scale required for two neighbouring atoms to interact.

After an ionization has occurred, one of the electrons is more deeply bound. Usually, the atom and the ion move apart with approximately equal velocities as discussed in the next section. An important quantity is the distribution of binding energies for the atom. A somewhat simpler representation uses the distribution of atoms as a function of the principal quantum number, n. The n distribution of atoms is plotted in figure 1 for the three heavier atoms. The n-state is given as a ratio relative to the initial n-state: $n_0 = 60$. Of course, the largest n-states allowed after the ionization have $n = n_0/\sqrt{2}$ since the final state of the atom must have at least twice the binding energy of the original atom.

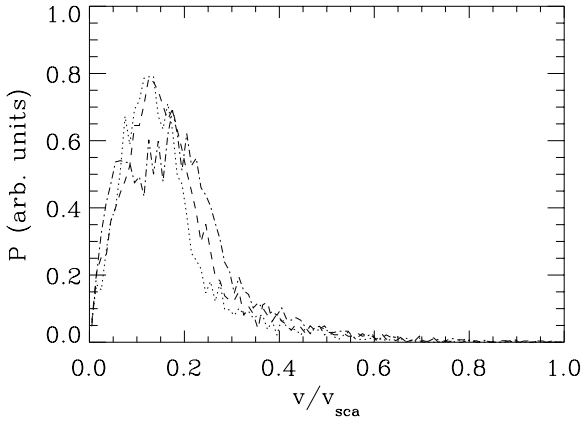

Figure 2. The distribution of velocity of the ions after penning ionization. The velocities have been scaled by $v_{\rm sca} \equiv \sqrt{2{\rm BE}/M}$ where BE is the original binding energy of the atom and M is the mass of the atom. The starting parameters and type of curves are the same as in figure 1. For $v = v_{\rm sca}/10$ the kinetic energy of the ion is 1% of the original binding energy of the atom. Because the atoms start with velocities much smaller than the final velocities, the final velocity of the atom is approximately equal and opposite that of the ion.

The distribution of final states displays some interesting features. The first is the similarity between the different atoms. This shows that the speed with which the atoms come together is slow enough that the electrons respond in similar ways for all atoms. This is not completely obvious because the ionization is a non-adiabatic event and the speed with which the atoms come together could influence the outcome. Another interesting feature is the dependence of the distribution on n. The distribution monotonically increases to the maximum allowed value of n because small energy changes are favoured in long-range Coulomb interactions. To get an idea about the n-dependence, a curve proportional to n^5 is also shown in figure 1. A curve proportional to n^6 gives slightly poorer agreement with the distribution in figure 1. We do not know why the distribution should be roughly proportional to such a high power of n, but we note that the final volume of space that the bound electron moves in is proportional to n^6.

5.2. Atom and ion velocities

After an ionization, the resulting atom and ion usually separate to extremely large distances. The typical trajectory of these three particles results in a pair of ions and an electron with a motion that gives a net repelling force between the two ions. Because the two atoms start with relatively small velocity, the relative velocity of the two ions is usually much larger than the centre of mass velocity of the ions. Because of this, the ion and atom have nearly equal and opposite velocities when they separate to large distance.

We plot the distribution of ion speeds scaled by the binding energy in figure 2; the scale speed $v_{\rm sca} = \sqrt{2{\rm BE}/M}$ where BE is the binding energy of an atom and M is the mass of the ion. As can be seen, the distribution is very similar for the different atoms. This shows that the internal dynamics (essentially governed by the motion of the electron) is very similar for the different atoms. Thinking of the motion of the ions as being adiabatic, we can imagine there is an effective potential between the two ions, $U_{\rm eff}(R)$, that depends on the trajectories. The relative velocity of the ion and atom will be determined by conservation of energy at large distances $(1/2)Mv^2 + U_{\rm eff}(R) = E$.

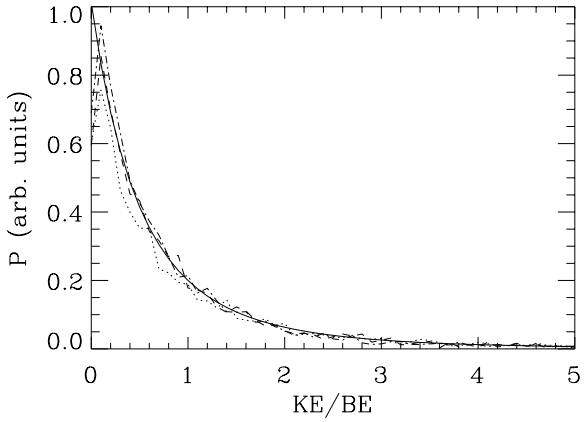

Figure 3. The distribution of kinetic energy of the ejected electron scaled by the original binding energy of the atom. The starting parameters and type of curves are the same as in figure 1. The solid line is proportional to $1/(\mathrm{KE}+2\mathrm{BE})^4$. Because little energy relative to the binding energy is in the final kinetic energy of the atom and ion, the kinetic energy of the electron is approximately determined by the final binding energy of the atom.

The velocity distribution in figure 2 can be converted into a kinetic energy distribution. Importantly, the peak of the kinetic energy distribution is at approximately $1/100$ of the original binding energy of an atom. Thus, only a small fraction of the binding energy is converted into translational motion of the atoms or ions. But even this small amount of energy is large compared to the original thermal energy of the atoms. For the parameters of the current simulation, the ion and atom have average speeds more than $10\times$ greater than the average thermal speed.

5.3. Kinetic energy of ejected electrons

In the previous section the distribution of atom and ion velocities were given. Converting the velocities into kinetic energies shows that approximately 1% or less of the initial binding energy is converted into the kinetic energy of the atom and ion. Thus, almost all of the energy lost by one electron is gained by the other electron. The distribution of kinetic energy of ejected electrons is directly obtained from the distribution of atomic levels of the atom. In that section, it was shown that the distribution of n-levels is roughly proportional to n^5 up to the maximum allowed n. The distribution of kinetic energies can be obtained from the distribution of n using $f(\mathrm{KE}) = f(n)\,\mathrm{d}n/\mathrm{d}E = n^8$. The kinetic energy and n are related through energy conservation

$$2\times\left(-\frac{1}{2n_0^2}\right) = -2\mathrm{BE} \simeq \mathrm{KE} + \left(-\frac{1}{2n^2}\right) \tag{6}$$

where BE is the binding energy of an atom and KE is the kinetic energy of the ejected electron. This gives a kinetic energy distribution approximately proportional to $1/(2\mathrm{BE}+\mathrm{KE})^4$ where BE is the binding energy of one atom. This expression will only be accurate for kinetic energy up to a few times the binding energy.

The kinetic energy distribution of the ejected electron is displayed in figure 3. The kinetic energy has been scaled by the original binding energy of an atom. We also plot a distribution proportional to the simplified expression $1/(2\mathrm{BE}+\mathrm{KE})^4$. It is clear that this simple expression gives a decent representation of the kinetic energy distribution. The region

of largest disagreement is very close to threshold where the CTMC distributions turn down. It is not clear whether this is a sampling bias in our definition of ionization in the CTMC calculation or is a real effect.

5.4. Molecular ions

After an electron is ejected, we propagate Hamilton's equations until either the separation of the atoms is 20% larger than the initial separation *or* for 1 μs. Oddly, we find that a few per cent of the trajectories reach the 1 μs limit without reaching a separation 20% larger than the initial separation. The percentage of molecules formed was larger for the heavier atoms. When we examined these trajectories, we found that the nuclei were vibrating. After the ionization transition, the two nuclei and the remaining electron were on a trajectory that gave bounded motion.

Some of these trajectories were characterized by an electron bound to one nucleus but with an attractive dipole that bound the other nucleus. For some of the trajectories, the electron oscillated around both nuclei in turns: when the nuclei were far apart the electron revolved around one and when the nuclei came close together it could revolve around both (which nucleus the electron became trapped on when the nuclei moved apart seemed to be random).

Many of the trajectories that survived to 1 μs appeared to be unstable; the motion did not repeat and the orbits became more erratic and larger with time. However, several trajectories appeared to be a relatively stable oscillation. This is consistent with the trend that more molecules formed for the heavier atoms: the heavier atoms would oscillate fewer times in 1 μs and would be more likely to survive.

For these molecular ions, all of the distances between the charged particles were roughly the original size of the atoms. It seems unlikely that it would be possible to observe these molecular ions. The ions are created in a region where there are many Rydberg atoms. Many Rydberg atoms will be attracted to the net positive charge of the molecular ion. The collision between the molecular ion and Rydberg atoms would undoubtedly destabilize the molecular ion. Although it seems improbable that a molecular ion could survive collisions with the background Rydberg gas, any surviving molecular ions would be easy to detect with time-of-flight techniques since they have mass $2M$ but charge e.

5.5. Van de Graaff transition

There were several trajectories for which the dipole–dipole interaction was initially attractive. After a time the atoms were accelerated towards each other and gained noticeable speed. But before the atoms reached the distance where ionization could occur, the non-Coulomb part of the potential caused the Runge–Lenz vector to precess into a different direction where the dipole–dipole interaction was repulsive. The atoms were then repelled apart. During such a trajectory, net positive work is done on the atoms on both the incoming and the outgoing parts of the trajectory. This is analogous to how a Van de Graaff accelerator works.

The energy gained by the atoms is a small fraction of the binding energy of the atoms (between $1/1000$ and $1/100$ of the binding energy). Since the original kinetic energy of the atoms can be much, much smaller than the binding energy, the energy gained due to this Van de Graaff mechanism can be substantially larger than the initial thermal energy of the atoms, providing a heating mechanism for the atoms.

I expect that this process also would be present in a quantum calculation. The quantum version would work through crossings of the internal energy levels as a function of the distance, R, between the atoms. At large R, the energy levels are degenerate. As R decreases,

the energy levels fan apart and levels associated with different n-manifolds can cross. At the crossing, the internal state can change character from giving attractive potential to giving a repelling potential. If the atom remains on the repelling potential, the internal levels will evolve into different n-manifolds. The smallest energy change would be for one atom to go to $n - 1$ and the other to go to $n + 1$. Such a state change corresponds to a decrease in the total internal energy of the two atoms given by $3/n^4$ atomic units (this energy change is $6/n^2$ of the binding energy of one atom).

6. Final remarks

We have generated data for the ionization due to the interaction between cold Rydberg atoms. We have computed the distribution of n-states, the distribution of atom and ion velocities, and the distribution of kinetic energies of the ejected electrons after the ionization. Although the ionization step is non-adiabatic, the distributions for different atoms are similar.

The collisions between cold Rydberg atoms result in several products that can strongly affect other Rydberg atoms. (1) Most of the electrons ejected in the ionization process have kinetic energies less than the original binding energy of the atom. Electrons with kinetic energy comparable to or less than the binding energy have extremely large inelastic scattering cross sections. (2) After the ionization both the ion and the resulting atom recoil with approximately 1% of the binding energy. This can be much larger than the original kinetic energy of the atoms. These atoms and ions can then collide with Rydberg atoms that have not yet been disturbed. (3) A Van de Graaf collision mechanism can transfer 0.1% to 1% of the binding energy into kinetic energy of the atoms. These atoms can have higher kinetic energy than the background Rydberg gas and can collide more frequently with the background atoms.

The products of the Rydberg–Rydberg collisions are themselves extremely effective at causing electronic transitions in Rydberg atoms. Thus, we expect that the electronic levels of a Rydberg gas will be substantially mixed soon after a small fraction, 1–10%, of the cold Rydberg atoms collide.

Acknowledgment

This work was supported by the NSF. Computational work was carried out at the National Energy Research Scientific Computing Center in Oakland, CA, USA.

References

[1] Fioretti A, Comparat D, Drag C, Gallagher T F and Pillet P 1999 *Phys. Rev. Lett.* **82** 1839
[2] Zanon R A D S, Magalhaes K M F, de Oliveira A L and Marcassa L G 2002 *Phys. Rev.* A **65** 023405
[3] de Oliveira A L, Mancini M W, Bagnato V S and Marcassa L G 2003 *Phys. Rev. Lett.* **90** 143002
[4] Walz-Flannigan A, Guest J R, Choi J-H and Raithel G 2004 *Phys. Rev.* A **69** 063405
[5] Olson R E 1979 *Phys. Rev. Lett.* **43** 126
[6] Burkhardt C E, Ciocca M, Leventhal J J and Kelley J D 1992 *Phys. Rev.* A **46** 5795
[7] Hahn Y 2000 *J. Phys. B: At. Mol. Opt. Phys.* **33** L655
[8] Robicheaux F, Hernández J V, Topçu T and Noordam L D 2004 *Phys. Rev.* A **70** 042703